

A Resistance-to-Digital Converter Possessing Exceptional Insensitivity to Circuit Parameters

A Project Report

submitted by

SEMEERALI.K

*in partial fulfilment of the requirements
for the award of the degree of*

MASTER OF TECHNOLOGY



**DEPARTMENT OF ELECTRICAL ENGINEERING
INDIAN INSTITUTE OF TECHNOLOGY MADRAS.**

MAY 2016

THESIS CERTIFICATE

This is to certify that the thesis titled **A Resistance-to-Digital Converter Possessing Exceptional Insensitivity to Circuit Parameters**, submitted by **Semeerali.k**, to the **Indian Institute of Technology, Madras**, for the award of the degree of **Master of Technology**, is a bona fide record of the research work done by him under our supervision. The contents of this thesis, in full or in parts, have not been submitted to any other Institute or University for the award of any degree or diploma.

Dr. Boby George
Research Guide
Associate Professor
Dept. of Electrical Engineering
IIT-Madras, 600 036

Place: Chennai

Date: 18th May 2016

ACKNOWLEDGEMENTS

I take this opportunity to express my sincere and deep sense of thanks and gratitude to my project guide Dr. Bobby George for his, excellent guidance, timely advice, constant encouragement and motivation throughout my project. It has been a very enriching and enjoyable experience to work under him

I am also extremely grateful to Prof. Jagadeesh Kumar V., Head, Measurement and Instrumentation Laboratory, IIT Madras for allowing me to have access to all the lab facilities that I needed from time to time for successful completion of the project. Also, his brilliant comments and suggestions during project progress review sessions proved priceless to me.

I take special pleasure in acknowledging research scholar Sreenath in the Measurements and Instrumentation Laboratory, for spending his invaluable time with me, in discussing about the project and answering my queries.

I would also like to thank all the teaching and non-teaching staff, especially Mr. B. Umaithanu Pillai, Mrs. Rekha of the Electrical Department for extending all the support and cooperation to me throughout.

I am also grateful to my lab mates, especially Gashay who shared his invaluable knowledge during the development of the android application for the project.

I also thank my friends Ramkumar, Gashay, Sudhir, Raja Paul, Vivek Gangadharan for the invaluable discussions and memorable times in the lab.

Last but not the least, I must not forget to thank Almighty for the wisdom and perseverance that He bestowed upon me during this project work.

ABSTRACT

KEYWORDS: Resistive sensor; resistance-to-digital converter (RDC); relaxation oscillator; insensitivity to circuit parameters

A new Resistance-to-Digital Converter (RDC) suitable for single element resistive sensors is presented. The proposed scheme is based on a relaxation oscillator circuit, which along with a timer-counter that measures the time intervals of oscillations, provides digital output proportional to the resistance of the sensor. In most of the existing RDCs, the output characteristic suffers from gain, offset and non-linearity errors owing to various circuit parameters and their drift in the measurement unit. The output of the proposed RDC has a special nature, by the design of the measurement method, that it is not a function of the circuit parameters such as offset voltages and bias currents of the opamps and comparators used, gain of various units employed, ON resistance of the switches, value or mismatch in the magnitudes of the reference voltages employed, etc. Such a scheme will be useful for high accuracy measurements, even in circumstances where the above-mentioned parameters may vary or drift, due to variation in the measurement environment, say, large variation in temperature.

A prototype of the proposed RDC has been developed in the laboratory and the performance has been tested under various conditions. The output was found to be linear with a worst-case non-linearity of 0.06 %. As expected, the sensitivity of output from the prototype RDC to various circuit parameters was found to be negligible.

TABLE OF CONTENTS

LIST OF TABLES	iii
LIST OF FIGURES	v
ABBREVIATIONS	vi
NOTATION	vii
1 INTRODUCTION	1
1.1 Resistive Sensors	1
1.2 OBJECTIVE AND SCOPE OF THE PROJECT	2
1.3 ORGANISATION OF THE THESIS	3
2 THE RESISTANCE-TO-DIGITAL CONVERTER	4
2.1 Description of the Circuit (Ideal Case)	4
2.2 Operation of the RDC	4
2.2.1 Cycle— R_x	5
2.2.2 Cycle— R_s	6
2.3 Operation of the Circuit (Practical Case)	7
2.4 Effect of the non-idealities on the operation of RDC	8
2.4.1 Effect of offset voltage and bias current of opamp	8
2.4.2 Effect of change in voltage gain G	9
2.4.3 Effect of mismatch in reference voltage V_R	10
2.4.4 Effect of ON resistance of Switch	10
3 DESIGN AND DEVELOPMENT OF THE CIRCUIT	12
3.1 Simulation studies	12
3.1.1 Arduino uno	13
3.1.2 HC-05 Bluetooth Module	14
3.1.3 Standalone ATmega 328P circuit	14

3.2	Android Application Development	15
3.2.1	Code Block	18
4	EXPERIMENTAL SETUP AND RESULTS	21
4.1	Description of prototype	21
4.2	Tests Conducted and the Results	24
4.3	PCB Design and Fabrication	27
4.4	Temperature test	27
5	CONCLUSION	29
5.1	SUMMARY OF THE WORK	29
5.2	FUTURE WORK	29
	REFERENCES	29
A	C-CODE FOR PROGRAMMING ATMEGA328 MICROCONTROLLER	32
B	PCB LAYOUT	38
B.0.1	TOP LAYER	38
B.0.2	BOTTOM LAYER	38

LIST OF TABLES

4.1	% error in reading	25
4.2	Effect of V_{OS1} and I_B	26

LIST OF FIGURES

2.1	Block diagram of the proposed Resistance to-Digital converter . . .	4
2.2	The wave forms at the output and the inverting terminal of integrator and comparator output of RDC, during cycle— R_x operation.	5
2.3	The circuit equivalent of RDC depicting the effect of input offset voltage of opamp V_{OS1} , bias current of opamp I_B and input offset voltage of comparator V_{OS2}	7
2.4	The circuit equivalent of RDC depicting the effect of ON resistance of switch	11
3.1	Simulation study of the proposed scheme	12
3.2	Simulation study graph of the proposed scheme	13
3.3	Interfacing Arduino with Bluetooth module	13
3.4	Stand alone atmega328p with arduino ISP	14
3.5	App Inventor start menu	16
3.6	App Inventor Designer section	16
3.7	App Inventor Viewer Screen	17
3.8	App Inventor Designer start menu	17
3.9	Application RDC	20
3.10	App inventor display	20
4.1	The circuit model of RDC <i>plotted using fritzing</i>	21
4.2	Screen-shot of the oscilloscope showing the comparator output v_C and integrator output v_{oi} of the opamp OA, from the prototype developed	22
4.3	Detailed circuit diagram	23
4.4	Experimental setup	24
4.5	Output and percentage error with change in resistance R_x	25
4.6	Snap-shot of the oscilloscope screen showing the comparator output v_C and integrator output v_{oi} when an offset voltage $V_{OS1} = -200mV$ and bias current $I_B = -100nA$ are applied to the prototype developed .	26
4.7	Components mounted on double layer PCB	27
4.8	Temperature test conducted in the laboratory	28

4.9	Lab View screen shot	28
-----	--------------------------------	----

ABBREVIATIONS

AFJ	Adaptive Frequency Hopping
ADC	Analog-to-Digital Converter
CMOS	Complementary Metal-Oxide Semiconductor
CLU	Control and Logic Unit
ELVIS	Educational Laboratory Virtual Instrumentation Suite
EDR	Enhance Data Rate
JFET	The junction gate field-effect transistor
MUX	Multiplexer
OPAMP	Operational Amplifier
RDC	Resistance to Digital Converter
SPP	Serial Port Protocol
SPDT	Single Pole Dual Throw
SPICE	Simulation Program for Integrated Circuit Emulation
SPST	Single Pole Triple Throw
VI	Virtual Instrument

NOTATION

C	Capacitance
R	Resistance
I	Current
V	Voltage
f	Frequency
k	kilo
M	Mega
m	milli
Ω	Ohm
Hz	Hertz
V_R	Reference Voltage
v_c	Comparator Output
v_{oi}	Integrator Output Voltage
v_{S1}	Control Signal for Switch S1
v_{S2}	Control Signal for Switch S2
R_{ON}	On Resistance
R_{OFF}	Off Resistance
T_C	Timer Clock Period
T_{ON}	On Time
T_{Off}	Off Time

CHAPTER 1

INTRODUCTION

1.1 Resistive Sensors

Resistive sensors have long-established high-performance characteristics, in the industrial and scientific community, for sensing numerous physical parameters including but not limited to temperature, pressure, strain, humidity, fluid flow and light intensity [1]. A resistive sensor can be either single element or differential type. Single element resistive type sensor, as the name denotes is composed of only one resistance, whose value changes in proportion to the parameter being sensed

Several methods to measure the resistance, of such sensors, have been reported starting from the conventional Wheatstone bridge-based schemes to the modern Resistance-to-Digital Converters (RDCs) in which a digital converter that directly accepts the element(s) of a sensor as input(s) and provides a digital outputs proportional to the physical quantity being sensed.

Compared to analog instrumentation system, digital instrumenting systems are having a lot of advantages with excellent processing power and user-friendly interfaces. To interface a sensor having an analog voltage or current output to a digital Instrumentation system a suitable analog-to-digital converter (ADC) is required, by using RDC based scheme this can be achieved. Some of the RDC based systems are based on RC oscillator and timer-counter [2], [3], while others rely on resistance to pulse-width conversion [4], resistance-to-time conversion [5], sigma delta [6], charge balancing type [7], [8] and direct interfacing of resistance to a microcontroller [9] methods for the measurement.

Even though these measurement methods work well in a typical operating environment, the output of most of the schemes mentioned above will be affected if there is any deviation in circuit parameters, from the designed value. For example. For a differential-type resistive sensor Owen suggested a direct resistance-to-digital converter (RDC), that requires four integration periods, i.e., T_A , T_B , T_C , and T_D [7]. (In his

method, T_A and T_C are set, whereas T_B and T_D are measured.) In Owen's method, the final output is computed as $\frac{T_B - T_D}{T_B + T_D}$. Thus, the output is obtained by subtracting one measured time period from another. Hence, large systematic errors may result, particularly when the difference between the two periods is very small.

Deviation in circuit parameters from the designed value are very often expected especially in industrial, automotive, space, environmental monitoring applications. For example the bias current of the opamps increases by a factor of 2.3 for every $10^\circ C$ rise in temperature [3], similar variation will occur in the offset voltage of the opamps, value of resistance of the resistors used in the circuit and ON resistance of the switch, gain of amplifiers, etc., with change in temperature. These changes will be reflected in the output, affecting the reliability of the reading

It will be invaluable if an RDC that is inherently insensitive to the circuit parameters and its variation on environmental parameters can be developed, such a novel RDC that guarantees high immunity to non-ideal parameters of the circuit and its variation is presented.

In addition to achieving an improved reliability in the output, . The proposed RDC, its operation, analysis on its sensitivity to circuit parameters, are discussed below. It is then followed by the details of the 1prototype RDC developed and results obtained from the same.

1.2 OBJECTIVE AND SCOPE OF THE PROJECT

The objective of the project is to design a low cost RDC for single element resistive sensor that guarantees high immunity to non-ideal parameters of the circuit and its variation.

The circuit can be interfaced to work with a wide range of industrial and non-industrial applications involving Resistive sensors. The microcontroller used in the circuit can be programmed to give the output in portable devices like mobile phone as well as in PC.

1.3 ORGANISATION OF THE THESIS

The Chapter-1 gives an introduction to Resistive sensors, their types and applications in industrial sector. It also elaborates various resistive sensors already existing and their drawbacks, the importance of having a linear sensor with output dependent only on the measurand.

The Chapter-2 discusses, in detail, the description and operation of the circuit. How the output of the proposed prototype is independent of the circuit parameters has been derived mathematically with related block diagram and graphs, as required.

Design and development of the circuit along with the miniaturization of the circuit by using Atmega standalone circuit has been elaborated upon in Chapter-3. The chapter also discusses how to make an application using MIT app inventor for the project is explained.

Chapter-4 explains details of the circuit prototypes developed in the lab along with the experimental results including the PCB design and temperature test of the prototype developed.

In Chapter-5, conclusions have been drawn on the present work and scope of the future work has been presented.

CHAPTER 2

THE RESISTANCE-TO-DIGITAL CONVERTER

2.1 Description of the Circuit (Ideal Case)

The block diagram of the proposed RDC is shown in Figure 2.1. R_x represents the resistive sensor whereas R_s is a fixed resistance whose value is known. The operational amplifier OA, feedback capacitor C_f comparator OC, SPDT switches S_1 and S_2 , and a stage with gain $G(=2, \text{ realized using a non-inverting amplifier})$ form a relaxation oscillator. Switch S_1 is controlled by the signal V_{S1} from the control and logical unit (CLU). S_2 will be connected to a reference voltage V_R if output v_c of OC is high, otherwise it will be connected to $-V_R$. The operation of RDC is explained below

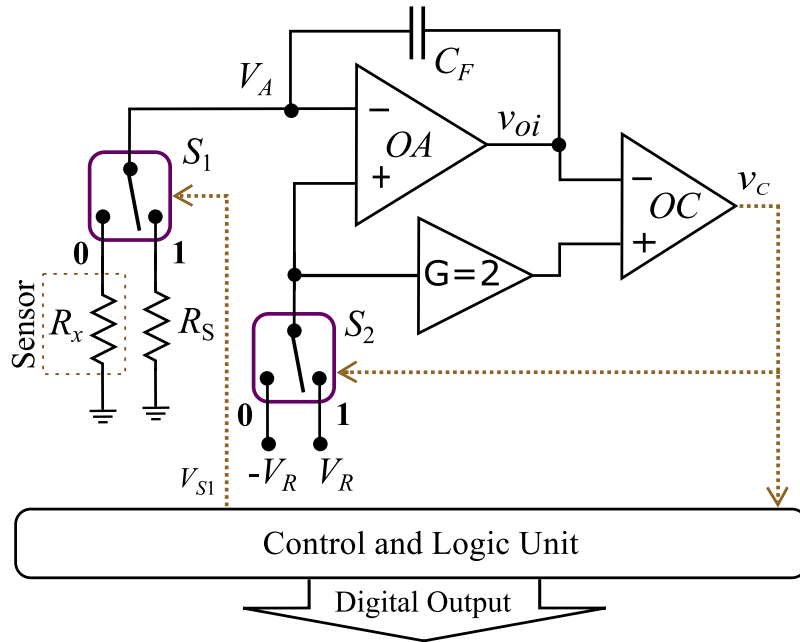


Fig. 2.1 Block diagram of the proposed Resistance to-Digital converter

2.2 Operation of the RDC

The RDC can operate in two modes, namely cycle- R_x and cycle- R_s . When S_1 is in position-0, the R_x will be active and the operation of the RDC during this condition is

called as cycle- R_x . If the CLU sets S_1 in position-1, R_x will be active instead of R_s . The operation of the circuit, in such a condition is named as cycle- R_s . Details of the operation of the RDC in these modes are described in the sections below.

2.2.1 Cycle- R_x

As mentioned earlier, S_1 will be kept at position-0 throughout the cycle- R_x . Initially, let us consider that the output v_c of OC is high. Then S_2 will be in position-1 and output of gain stage G will be $2V_R$. In this condition, the integrator voltage v_{oi} will be less than $2V_R$. In this switch position, the voltage V_A will be V_R and there will be a current $\frac{V_R}{R_x}$ flowing through the sensor. This will charge the capacitor C_F and the voltage v_{oi} will increase with time in a positive direction as shown in Figure(2.2). When the voltage v_{oi} reaches $2V_R$, the output of the comparator turns LOW which sets S_2 to 0. As soon as v_c turns low, output of gain stage G will become $-2V_R$ and voltage V_A at

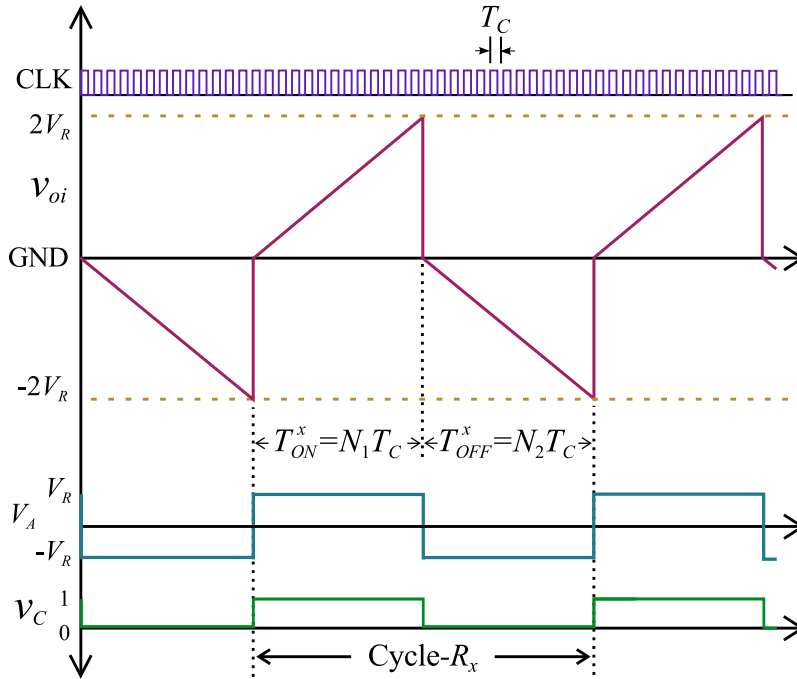


Fig. 2.2 The wave forms at the output and the inverting terminal of integrator and comparator output of RDC, during cycle- R_x operation.

the inverting terminal of the opamp will be $-2V_R$. Thus, there will be a current $\frac{-V_R}{R_x}$ flowing through the R_x , which discharges C_F and results in a gradual decrease in the voltage v_{oi} , with time. This will continue until v_{oi} reaches $-2V_R$. Once this condition occurs, the comparator will change its state from LOW to HIGH and sets S_2 to position-

1. This is same as the initial condition we assumed to begin the discussion on operation of the circuit. Thus, now the circuit will operate as explained earlier and continue until there is a transition in v_c . This shows that the circuit shown in Figure 2.2, is a relaxation oscillator. Let us name the duration for which v_c is high as an ON period T_{ON}^x and the interval when v_c is low as OFF period T_{OFF}^x . This is illustrated in Figure 2.2. Then, the time intervals T_{ON}^x and T_{OFF}^x can be represented as in (2.1). In an ideal situation, the magnitude of change in v_o , during T_{ON}^x and T_{OFF}^x is equal to $2V_R$, thus T_{ON}^x and T_{OFF}^x are equal as seen from (2.1). In a practical case, these intervals will be unequal; the details are discussed later in this section.

$$T_{ON}^x = T_{OFF}^x = 2R_x C_F \quad (2.1)$$

The time intervals T_{ON}^x and T_{OFF}^x can be measured using the counter in the CLU. Let us say that the timer is operating from a clock at $\frac{1}{T_C}$ Hz. Then, the counter output N_1 at the end of T_{ON}^x will be $N_1 = \frac{T_{ON}^x}{T_C}$. Similarly, the count N_1 during T_{OFF}^x will be $N_2 = \frac{T_{OFF}^x}{T_C}$.

2.2.2 Cycle— R_s

To perform cycle- R_s measurement, the CLU will set S_1 to position-1 and keep in that condition throughout the cycle- R_s . The operation of the circuit will remain same except that the charging and discharging currents are now $\frac{V_R}{R_s}$ and $-\frac{V_R}{R_x}$ respectively. In this case, the ON period and OFF period are denoted as T_{ON}^S and T_{OFF}^S respectively. The same counter can be used to count these intervals. Let the corresponding counts be $N_3 = \frac{T_{ON}^S}{T_C}$ and $N_4 = \frac{T_{OFF}^S}{T_C}$ in order. The operation of the RDC is explained assuming ideal components and ICs, but in reality there will be a number of non-idealities present, which could affect the operation. In order to explain the effect of various circuit parameters, Figure 2.1 has been modified incorporating some of the non-idealities, such as offset voltage of opamp, bias current of opamp and offset voltage of comparator and presented in next section.

2.3 Operation of the Circuit (Practical Case)

The block diagram of the proposed RDC by considering offset voltage of opamp, bias current of opamp and offset voltage of comparator is shown in Figure 2.4. For ease of

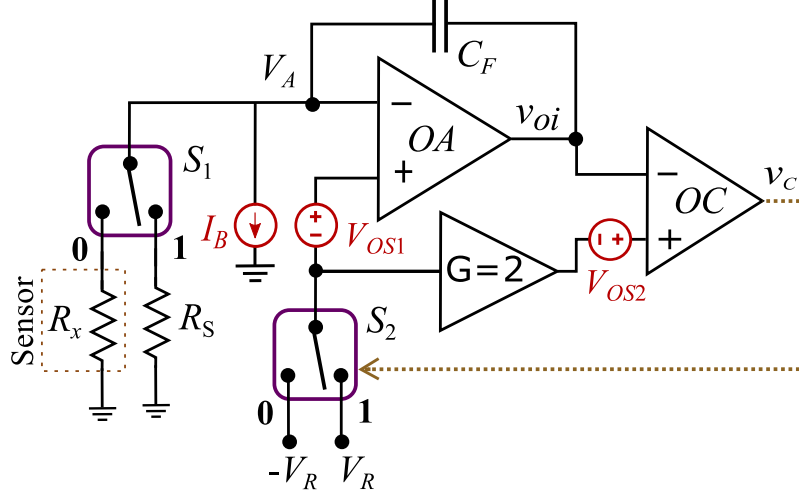


Fig. 2.3 The circuit equivalent of RDC depicting the effect of input offset voltage of opamp V_{OS1} , bias current of opamp I_B and input offset voltage of comparator V_{OS2}

explanation, the effect of other circuit parameters such as mismatch in reference voltage, variation in the gain G , ON resistance of switch etc. are discussed later. The effect of each parameter on the operation of RDC is discussed and analyzed below. A method to compute the output which is insensitive to these circuit parameters is also presented

The comparator can have an input offset voltage V_{OS2} , as a result of this, the comparator OC will monitor v_{oi} with respect to $(2V_R + V_{OS2})$ and $(-2V_R + V_{OS2})$ when switch S_2 is at position 1 and 0, respectively. When S_2 switches from 1 to 0, the output voltage of opamp v_{oi} will change from $(2V_R + V_{OS2})$ to V_{OS2} , whereas when S_2 switches from 0 to 1, the voltage v_{oi} will change from $(-2V_R + V_{OS2})$ to V_{OS2} . Thus, the net change in voltage in v_{oi} during T_{ON} and T_{OFF} remains the same, i.e., $2V_R$. Thus, the input offset voltage of comparator V_{OS2} will not affect the operation of RDC.

Let V_{OS1} be the input offset voltage of opamp OA. Now, during T_{ON}^x there will be an additional current $\frac{V_{OS1}}{R_s}$ flowing through R_x along with the ideal current $\frac{V_R}{R_x}$. Similarly, an additional current of $\frac{V_{OS1}}{R_s}$ will be present throughout the cycle- R_s . Thus, the offset voltage V_{OS1} will increase the output voltage of opamp v_{oi} by $\frac{V_{OS1}T_C}{C_F R_x}$ and $\frac{V_{OS1}T_C}{C_F R_s}$ after

each clock cycle during cycle- R_x and cycle- R_S respectively

Let I_B be the bias current flowing from the inverting terminal of opamp OA, as depicted in Figure 2.4. This bias current I_B will flow through the feedback capacitor throughout the cycle- R_x as well as cycle- R_S . This results in an incremental voltage change in v_{oi} by $\frac{I_B T_C}{C_F}$ after each clock cycle during the operation of cycle- R_x as well as cycle- R_S

2.4 Effect of the non-idealities on the operation of RDC

2.4.1 Effect of offset voltage and bias current of opamp

In order to analyze and quantify the effect of V_{OS1} and I_B , the contribution of these parameters are incorporated in the charge balancing condition that the total (sum of the) charge during the ON and OFF period is zero. This condition comes from the fact that the change in v_{oi} during ON as well as OFF are equal and opposite. In an ideal case, during the ON period of cycle- R_x , the change in voltage in v_{oi} in one clock cycle (period T_C) is $\frac{V_R T_C}{R_x C_F}$ and during OFF period, it will be $\frac{-V_R T_C}{R_x C_F}$. Thus, the charge balance or voltage balance equation, in an ideal condition, for cycle- R_x can be represented as in (2.2). N_1 and N_2 are the counter outputs during ON and OFF periods, respectively. As discussed above, with the presence of V_{OS1} and I_B , (2.2) will get modified as (2.3).

$$N_1 \left[\frac{V_R T_C}{R_x C_F} \right] + N_2 \left[\frac{-V_R T_C}{R_x C_F} \right] = 0 \quad (2.2)$$

$$N_1 \left[\frac{(V_R + V_{OS1}) T_C}{R_x C_F} + \frac{I_B T_C}{C_F} \right] + N_2 \left[\frac{(-V_R + V_{OS1}) T_C}{R_x C_F} + \frac{I_B T_C}{C_F} \right] = 0 \quad (2.3)$$

By rearranging (2.3), we get (2.4)

$$-\left(\frac{V_{OS1} T_C}{R_x C_F} + \frac{I_B T_C}{C_F} \right) = \left(\frac{N_1 - N_2}{N_1 + N_2} \right) \left(\frac{V_R T_C}{C_F R_x} \right) \quad (2.4)$$

Now, the net change $2V_R$ in voltage v_{oi} during the ON period of cycle- R_x can be represented as

$$N_1 \left[\frac{V_R T_C}{R_x C_F} + \left(\frac{V_{OS1} T_C}{R_x C_F} + \frac{I_B T_C}{C_F} \right) \right] = N_1 \left[\frac{V_R T_C}{R_x C_F} \left(1 - \frac{N_1 - N_2}{N_1 + N_2} \right) \right] = 0 \text{ or}$$

$$\left[\frac{2N_1 N_2}{N_1 + N_2} \right] \left[\frac{V_R T_C}{C_F R_x} \right] = 2V_R \quad (2.5)$$

In a similar approach, for cycle— R_x , (2.3) will get modified as given below.

$$N_3 \left[\frac{(V_R + V_{OS1}) T_C}{R_x C_F} + \frac{I_B T_C}{C_F} \right] + N_4 \left[\frac{(-V_R + V_{OS1}) T_C}{R_x C_F} + \frac{I_B T_C}{C_F} \right] = 0$$

By rearranging this equation, the net change in v_{oi} during the ON period of cycle— R_S can be obtained as in (2.6)

$$\left[\frac{2N_1 N_2}{N_1 + N_2} \right] \left[\frac{V_R T_C}{C_F R_x} \right] = 2V_R \quad (2.6)$$

From (2.5) and (2.6), the sensor resistance R_x can be found using (2.7)

$$R_x = \left[\frac{2N_3 N_4}{N_3 + N_4} \right] \left[\frac{N_3 + N_4}{N_3 N_4} \right] R_S \quad (2.7)$$

As can be seen from (2.7), the measurement of R_x from the RDC is independent of the non-idealities of the circuit elements such as offset voltage and bias currents of the opamps. Earlier it was shown that offset voltage of the comparator has no effect in the ON and OFF periods. Thus, using the measured counts N_1 , N_2 , N_3 and N_4 , and known resistance R_S , the unknown R_x can be obtained as in (2.7), which is independent of various circuit parameters as mentioned.

2.4.2 Effect of change in voltage gain G

So far in the operation, it was assumed that $G = 2$. In practice, it need not be exactly this value, or with temperature, this may get change. Let us consider that $G = 2k$; the new gain of the system. Thus, the comparator OC will now monitor the voltage v_{oi} with respect to $2kV_R$ and $2kV_R$ when the switch S_2 is positioned at 1 and 0, respectively. During the operation of RDC, when the switch S_2 changes its position from 1 to 0, the voltage v_{oi} will suddenly drop from $2kV_R$ to $2kV_R$. Similarly, a voltage change of $2kV_R$ to $2(k-1)V_R$ is expected at v_{oi} when S_2 turns from 0 to 1. Thus, even if the gain is different (can be higher or lower than 2), the magnitude of voltage change in v_{oi} during ON and OFF periods remains equal, i.e., $(2k-1)2V_R$. This is valid for cycle— R_x and

cycle— R_S . Since the magnitude of voltage change during the ON and OFF periods of cycle— R_x and cycle— R_S are still the same, the equations (2.5) and (2.6) are still valid except that their magnitude has changed from $2V_R$ to $(2k - 1)2V_R$. Thus, the sensor resistance R_x computed using (2.7) is not affected even if the voltage gain G change from 2 to $2k$.

2.4.3 Effect of mismatch in reference voltage V_R

A mismatch in the magnitudes of the reference voltage, V_R and $-V_R$ can be represented as aV_R and bV_R respectively. The modified reference voltages can be represented as in (2.8) and (2.9)

$$aV_R = V_D + V_{CM} \quad (2.8)$$

$$-bV_R = -V_D + V_{CM} \quad (2.9)$$

where $V_D = V_R \left(\frac{a+b}{2} \right)$ and $V_{CM} = V_R \left(\frac{a-b}{2} \right)$

A careful look into (2.8) and (2.9) suggest that the effect of voltage V_{CM} in the opamp input is equivalent to an input offset voltage $V_{OS1} = V_{CM}$, for OA. Similarly, its effect in the input of OC is equivalent to an input offset voltage $V_{OS2} = GV_{CM}$. In the earlier sections, it has been shown that the digital outputs of the RDC are insensitive to the offset voltage of opamp and comparator. Thus, the term V_{CM} will not introduce error except that the new reference voltage during the RDC operation will be equivalent to V_D and $-V_D$. As in (2.7), the sensor resistance R_x is independent of the magnitude of the reference voltage V_R . Hence V_R can be equal to V_D . Thus, the operation of the RDC is insensitive to the mismatch in the magnitudes of the reference voltage.

2.4.4 Effect of ON resistance of Switch

Since, the current through S_2 is zero, the ON resistance of S_2 will not influence to operation of RDC. Let R_{ON} be the ON resistance of S_1 . The presence of R_{ON} will modify (2.7) as

$$R_x + R_{ON} = \left[\frac{N_1 N_2}{N_1 + N_2} \right] \left[\frac{N_3 + N_4}{N_3 N_4} \right] (R_x + R_{ON}) \quad (2.10)$$

Equation (2.10) indicates that there will be an effect due to R_{ON} . To avoid the dependence of R_{ON} a slight modification can be introduced in the circuit. The S_1 can be replaced with a single pole triple throw (SPTT) switch and an additional fixed resistor R_C of known value can be introduced to the third terminal as shown in Figure 2.4. This

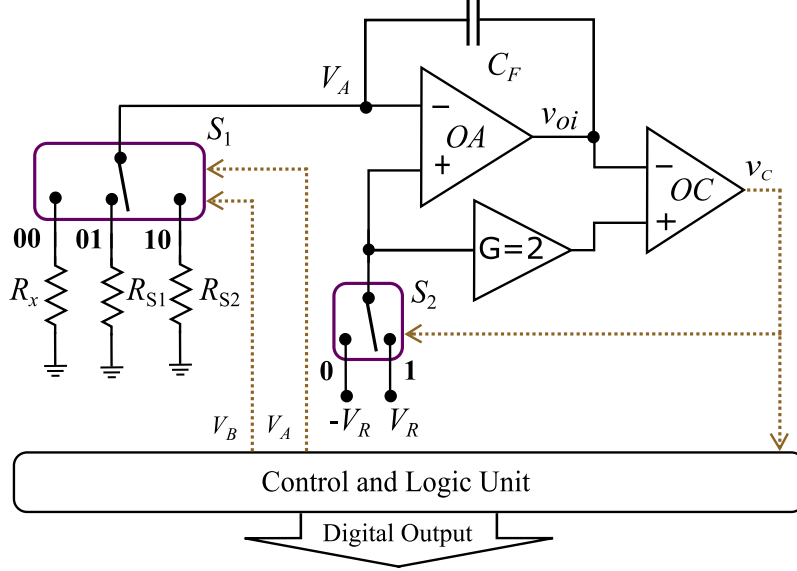


Fig. 2.4 The circuit equivalent of RDC depicting the effect of ON resistance of switch

switch can be implemented using a 4×1 multiplexer IC. Now, the circuit can operate by using R_x or R_S or R_C . A cycle- R_C operation can be introduced in the similar fashion of cycle- R_x (S_1 will be connected to R_C) to obtain the corresponding ON and OFF counts N_5 and N_6 . Thus, as in (2.10), we get

$$R_C + R_{ON} = \left[\frac{N_5 N_6}{N_5 + N_6} \right] \left[\frac{N_3 + N_4}{N_3 N_4} \right] (R_S + R_{ON}) \quad (2.11)$$

Since, R_C and R_S are known, the ON resistance R_{ON} can be found from (2.11). Since R_{ON} can be obtained from (2.11), and used in (2.10), the sensor resistance R_x can be measured accurately. For the prototype developed, the fixed resistance values chosen are $R_C = 30.27 \text{ k}\Omega$ and $R_S = 20.14 \text{ k}\Omega$ and MAX4709 IC was used to serve the purpose of SPTT switch S_1 . The ON resistance R_{ON} measured using the developed prototype was 442Ω . The cycle- R_C need not be performed continuously, instead it can be run once when the converter starts and then the corresponding R_{ON} can be stored. Same is valid for cycle- R_S . If the measurement environment (say temperature) is expected to change a lot while in use, these cycles can be performed on a regular basis by the CLU and output can be corrected, as discussed.

CHAPTER 3

DESIGN AND DEVELOPMENT OF THE CIRCUIT

3.1 Simulation studies

To test the functionality of the proposed scheme Figure 2.1 a SPICE based simulation (LT-SPICE) study was performed. Instead of giving the control signal from micro-controller a square wave given as the input to the SPDT switch. The circuit diagram of the same is shown figure 3.1. In order to switch between $+V_R$ and $-V_R$ SPDT switch U_4 is used and to switch between R_x and R_s SPDT switch U_6 is used. For a fixed value of R_s , R_x is varied.

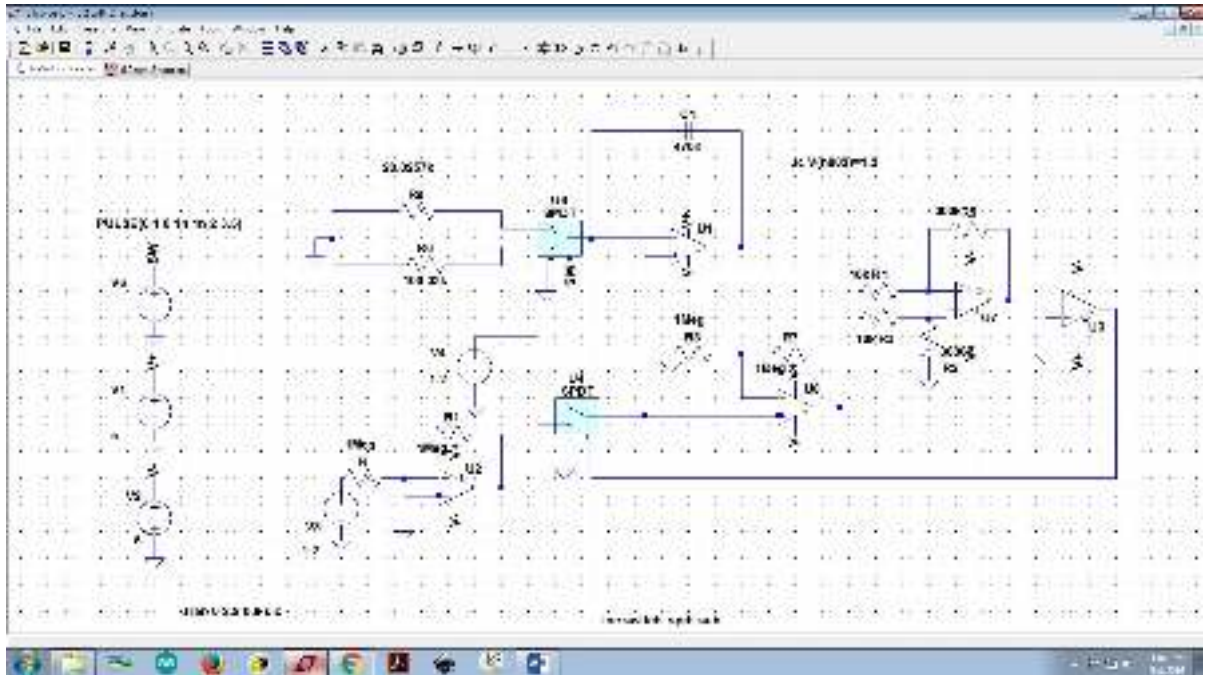


Fig. 3.1 Simulation study of the proposed scheme

The waveform obtained for the same is for a particular value of R_s , and R_x shown in figure 3.2, where $V(n002)$ is the output of the integrating opamp and $V(n009)$ is that of voltage follower.

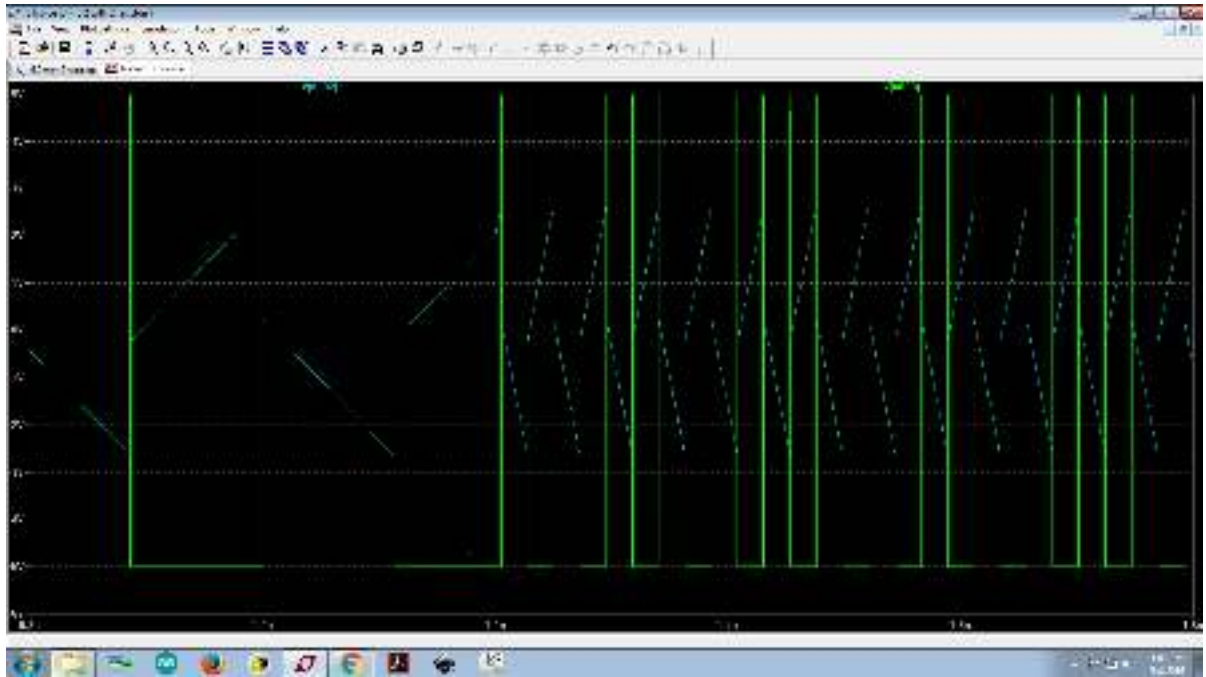


Fig. 3.2 Simulation study graph of the proposed scheme

3.1.1 Arduino uno

Arduino Uno board was used for the digitalization of sensor output. Due to its robustness and open source nature, it is interfaced with the Bluetooth module easily as shown in figure 3.3 . The Arduino Uno board has a microcontroller based on ATmega328P. This board provides the services of serial communication for displaying the received data on the android device and provides an Integrated Development Environment for easy programming.

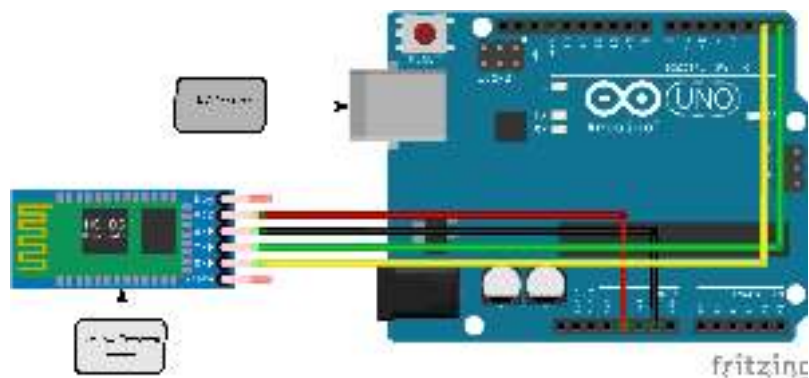


Fig. 3.3 Interfacing Arduino with Bluetooth module

3.1.2 HC-05 Bluetooth Module

HC-05 module is an easy to use Bluetooth SPP (Serial Port Protocol) module, designed for transparent wireless serial connection setup. Serial port Bluetooth module is fully qualified Bluetooth V2.0+EDR (Enhanced Data Rate) 3Mbps Modulation with complete 2.4GHz radio transceiver and baseband. It uses CSR Blue core 04-External single chip Bluetooth system with CMOS technology and with AFH(Adaptive Frequency Hopping Feature). It has the footprint as small as 12.7mmx27mm

HC-05 is a 6 pin IC where the TX and RX pin is connected to the RX and TX pin of the Arduino board respectively. We can use the voltage supply required for this HC-05 from the Arduino potential 3.3V for proper transmission and reception between the Arduino and the Bluetooth Module. We have to make sure that the baud rate of the Bluetooth module is synchronized with that of the Arduino so that there is no loss of data and proper communication is achieved.

3.1.3 Standalone ATmega 328P circuit

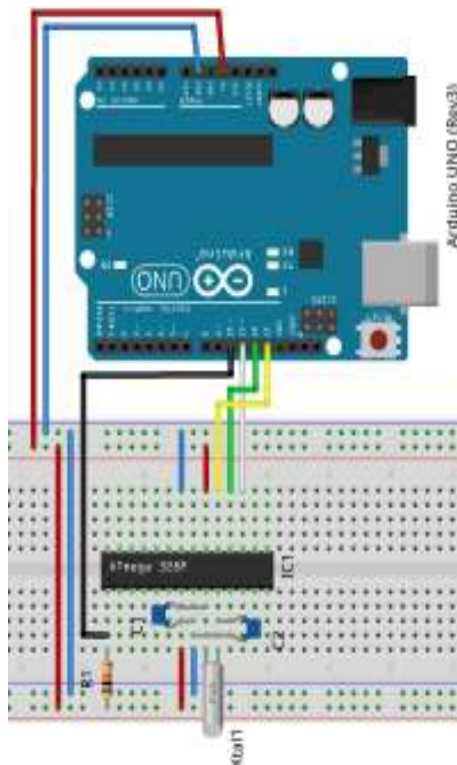


Fig. 3.4 Stand alone atmega328p with arduino ISP

The minimal standalone ATmega 328P circuit with external crystal from the ArduinoISP Tutorial is as shown in figure 3.4. Once the standalone ATmega 328P has been flashed to our satisfaction(after boot loading the microcontroller), we can disconnect the Arduino ISP. For programming the microcontrollers, the Arduino project provides an integrated development environment (IDE) based on a programming language named Processing, which also supports the languages C and C++, the microcontroller programmed using this software as per requirement.

For displaying the sensor output after removing the Arduino from the circuit an application was developed using App Inventor for which is explained in next section.

3.2 Android Application Development

App Inventor for Android is an open-source web application originally provided by Google, and now maintained by the Massachusetts Institute of Technology (MIT).It allows newcomers to computer programming to create software applications for the Android operating system (OS). It uses a graphical interface, very similar to Scratch and the Star Logo TNG user interface, which allows users to drag-and-drop visual objects to create an application that can run on Android devices. In creating App Inventor, Google drew upon significant prior research in educational computing, as well as work done within Google on online development environments. Following steps are used to develop the RDC app.

After login to the system using a Google ID, from the App Inventor Designer menu, start new project by clicking on new project as shown in Figure3.5

Enter **RDC** as a project name and click OK to continue. At this point, the App Inventor designer is showing 4 separate sections Palette, Viewer, Components and Properties as shown on Figure3.6

- **Palette:** This section contains different components which you can drag onto the Viewer to add them to your application. This is a familiar feature to the .NET developer.
- **Viewer:** This section provides a preview screen for your application where you can drag and drop components from the Palette section onto the screen and arrange the components to see how your app will look like.



Fig. 3.5 App Inventor start menu

- **Components:** This section lists all of the components that are added to your application. By clicking on a component, the selected component's properties are shown on the Properties section.
- **Properties:** This section displays all of the properties associated with a selected component and provides the interface for you to edit and change the setting or value for each of these properties.

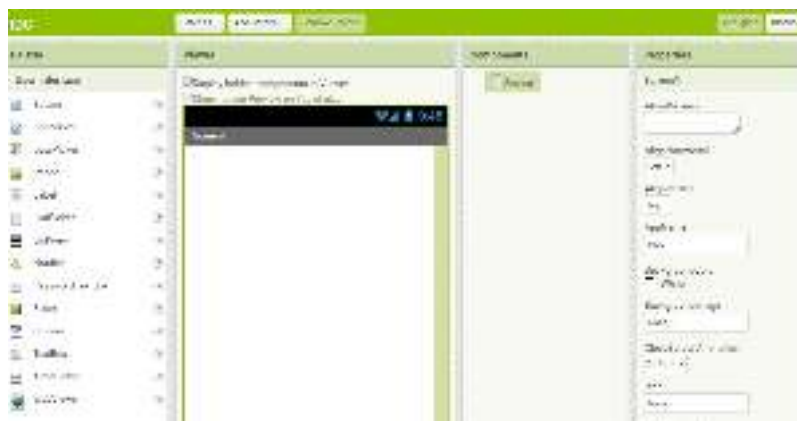


Fig. 3.6 App Inventor Designer section

From the Palette section, select and drag the *Label* component to the Viewer section **Sensor value...** as *Label1* name that used to display the resistance value. From the same section, select and drag the *ListPicker1* and *Button1* to the viewer section **connect Bluetooth** and **disconnect Bluetooth** as the name of *ListPicker1* and *button1* respectively. To the immediate right of the Android screen is a list of the current screen components: a *Label1*, *ListPicker1*, *Button1* and *horizontal arrangement*. There is also a non-visible components like Bluetooth client, clock and player1 at the bottom of the screen. To the far right of the Android screen are the properties of the currently selected component - in this case the Screen1 is selected, On the left of the screen is a list of

the components which can be dragged and dropped onto the Android screen, finally the screen will look like as shown in figure3.7 If we click on the Blocks Tab for instance,



Fig. 3.7 App Inventor Viewer Screen

click on the *ListPicker1* component on the left hand side of the screen. A scrollable list of code blocks relevant to the *ListPicker1* appears. Click on *When ListPicker1 Before Picking* and it will be placed onto the Blocks screen area as shown on figure3.8 We can

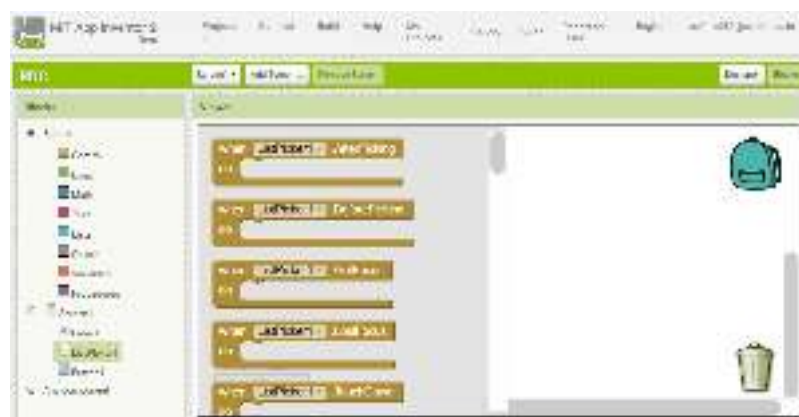


Fig. 3.8 App Inventor Designer start menu

now select further sub-Blocks to create the first full code Block.

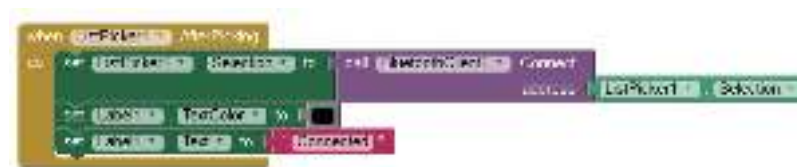
3.2.1 Code Block

3.2.1.1 Connecting Bluetooth

When the two devices are running, the server app is set up first to accept connections. Then, on the client side, the user selects the Connect *ListPicker1* button and selects the device name from a list of available Bluetooth devices. Because the list of devices is in the form of a list, the *ListPicker1* is a great interface component to display the device list and handle the selection. In general this allows *ListPicker1* to display the available (already paired) Bluetooth devices.



The next Block allows *ListPicker1* to select and connect to the desired Bluetooth device and to set the hidden Label, *Label1* to read CONNECTED.



We have then set the default Text of *Label1* to be Disconnected and the colour of *Label1* to be Red in the Design Screen; clearly, *Label1* is now no longer hidden. We have also added a further component into the code Block, to set the Text colour of *Label1* to be Black when the Bluetooth client is connected. After selecting paired Bluetooth we can check whether the device is connected or not by clicking on connected Bluetooth the hidden label, *Label1* to read connected.

3.2.1.2 Connecting Bluetooth

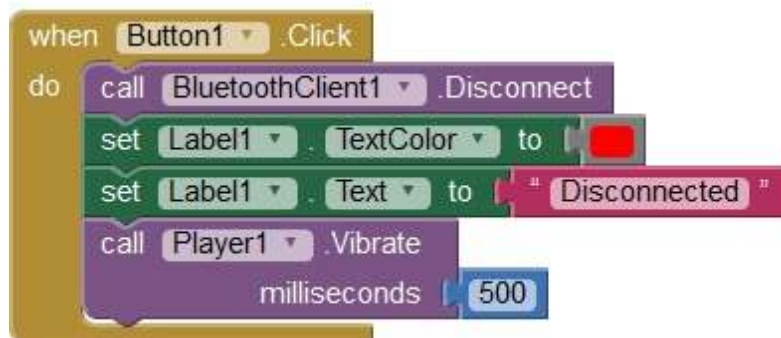
The reception of data is implemented using a timer. Once per second, the client checks to see if data is available, and if it is, reads and displays the data on the app display. After the device has been selected, with the *ListPicker* (Bluetooth connect) user interface, the



Connect method of *BluetoothClient1* establishes the connection. The method returns a value of true if the connection was successful; in which case a message is sent to the server app. The data is sent to android device is displayed

3.2.1.3 Disconnecting Bluetooth

Finally, we have added the Button1 in the Design screen with a Text value of Disconnect Bluetooth and a fourth Block of code which disconnects the Bluetooth client, sets *Label1* text colour to Red and *Label1* text to read Disconnected. We have also added a further component Player1 into the code Block, to set the 500ms vibration of Android device when the Bluetooth client is Disconnected. To disconnect the android device



and Bluetooth client simply click on the Disconnect Bluetooth button, the Clock component stop receiving data and *Label1* will show the Disconnected message. The screen on the mobile will look like as shown 3.10, in which two buttons are there to connect and disconnect the Bluetooth device

Before you use the Bluetooth communications apps, do the following :

1. Use Build .apk or other method to obtain the server app, download and install on your first Android device as figure 4.9 shown below
2. Go in to the Android Settings and turn on the Bluetooth feature. The user interface for the Bluetooth configuration varies slightly depending on which version of Android you have. For example, on Android 5.0, Bluetooth appears in the topmost Settings menu.



Fig. 3.9 Application RDC



Fig. 3.10 App inventor display

3. In newer versions of Android, when the Bluetooth Settings menu is active, your device is broadcasting its availability to other nearby devices. On older versions, you may need to click an option to make your device discoverable. .
4. Once your two devices see each other over Bluetooth, you may be prompted to pair the devices, or (depending on Android version), you may have to manually choose the device and then choose pairing. Follow the on screen instructions
5. Once the two devices are paired, launch the Server app and select Bluetooth device.
6. If we want to check whether the device is connected or not click on Bluetooth connect and Connected message is displayed on the screen.
7. Final we can install .apk file to any android device show in Figure 3.9 as name RDC.

CHAPTER 4

EXPERIMENTAL SETUP AND RESULTS

4.1 Description of prototype

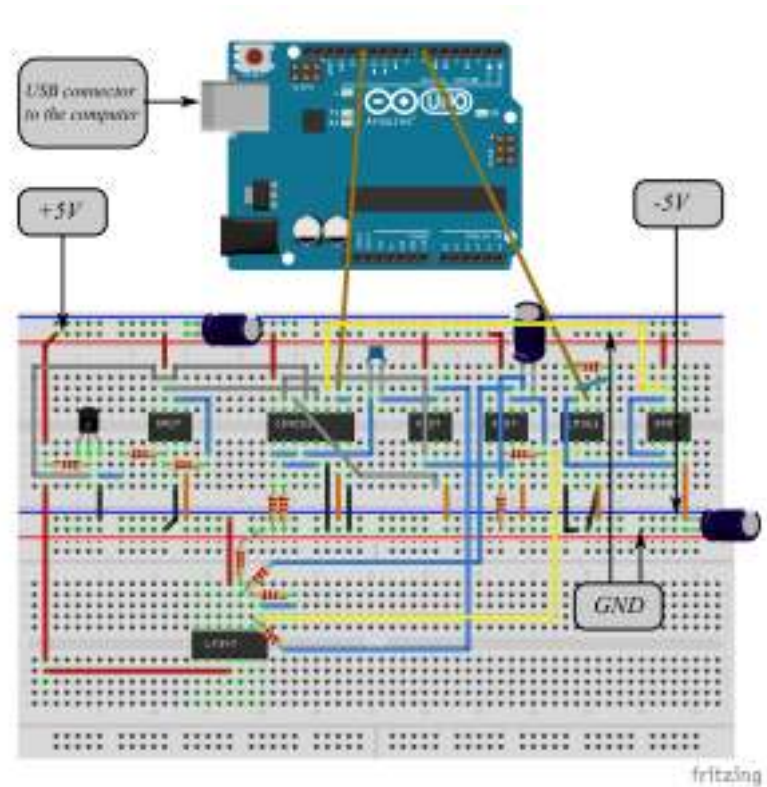


Fig. 4.1 The circuit model of RDC *plotted using fritzing*

After the simulation the prototype of the RDC, shown in figure 2.1 was developed and tested as shown in figure 4.1.. In the circuit, LM385-1.2N IC (micro-power Zener Diode Voltage Regulator IC) was used to set V_R as 1.2 V. An inverting amplifier was used to derive $-V_R$ from V_R . OP07 IC and The LM-311(low input current comparator IC) were used to realize opamp OA and comparator OC, respectively. In order to increase the accuracy of the time period measured by the controller, LF147 opamp is used before the comparator OC and the positive terminal of OC is grounded. (The LF147 is a low cost, high speed quad JFET input operational amplifier with an internally trimmed

input offset voltage. The device requires a low supply current and yet maintains a large gain bandwidth product and a fast slew rate).

These ICs were procured from Texas Instruments Inc. A 4×1 MUX MAX4053 was configured as SPDT switches S_1 and S_2 , later S_1 was replaced with SPTT switch MUX MAX4709. A non-inverting amplifier was used to set the voltage gain G as 2. In the RDC developed, the value of feedback capacitor $C_F = 470$ nF and fixed resistors employed were $R_S = 20.14k\Omega$ and $R_C = 30.27k\Omega$. The resistive sensor was emulated using a $1M\Omega$ potentiometer. The power supply of $5V$ required was tapped from the on-board variable power supply of the ELVIS II Board.

The resistance measured using the prototype RDC was compared using $6\frac{1}{2}$ -digit multi-meter, Agilent 34410A. The CLU was realized using an 8-bit microcontroller ATmega328. The operating frequency of the clock $\frac{1}{T_c}$ was set as 1 MHz. A suitable program to implement the necessary control logic to control S_1 , use the counter to measure the ON and OFF periods and calculate the output as per (2.7) and correct for the effect of R_{ON} using (2.11) and (2.10) was developed and burn into the microcontroller.

A snapshot of the waveform obtained from the prototype(4.4)., for sensor resistance $R_x = 9.78k\Omega$, is shown in figure4.2. The corresponding counts observed during cycle— R_x was $N_1 = 10962$ and $N_2 = 10734$.

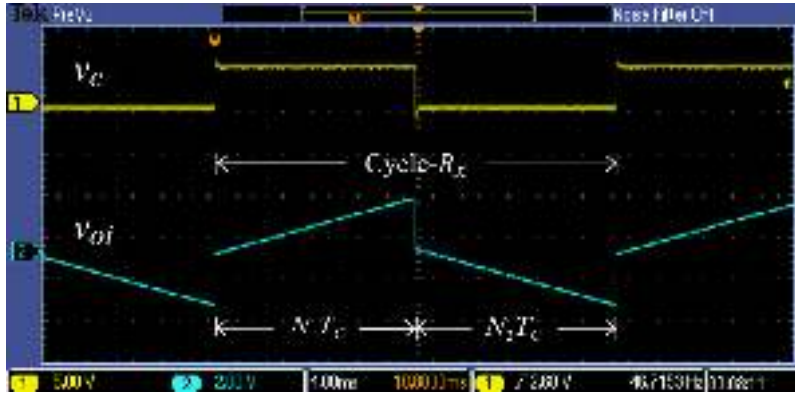


Fig. 4.2 Screen-shot of the oscilloscope showing the comparator output v_C and integrator output v_{oi} of the opamp OA, from the prototype developed

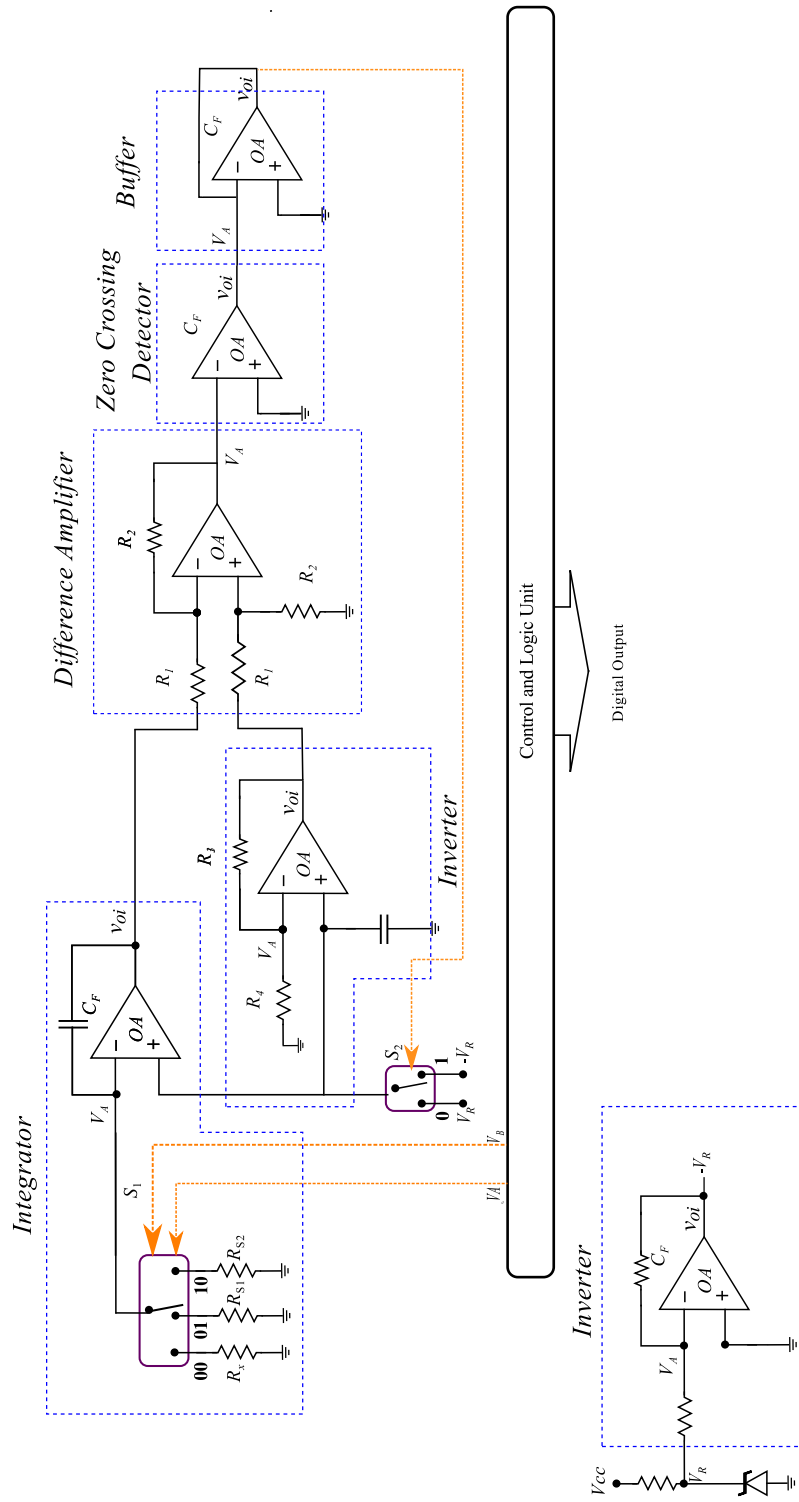


Fig. 4.3 Detailed circuit diagram

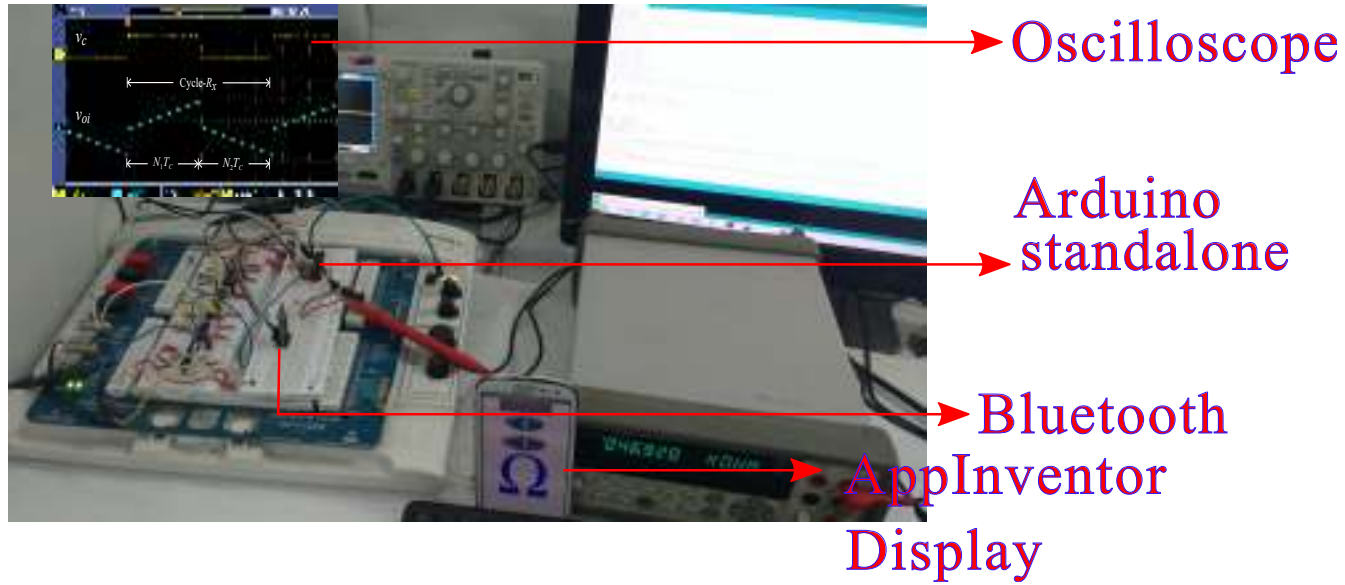


Fig. 4.4 Experimental setup

Detailed circuit diagram is shown in figure(4.3) and the complete experimental setup is shown in figure(4.4).

4.2 Tests Conducted and the Results

A linearity test was performed in the first stage of experiment. The cycle- R_S was performed initially, and the counts $N_3 = 22083$ and $N_4 = 21593$ for the fixed resistor $R_S = 20.14k\Omega$ were obtained. Then cycle- R_C was performed keeping $R_C = 30.27\Omega$ and the counts N_5 and N_6 were noted. From these, the R_{ON} was computed as 442Ω . Then, the sensor resistance R_x was varied from $1k\Omega$ to $220k\Omega$. The output from the prototype was compared with the actual values. From the measured values, a linearity analysis has been performed shows in table(4.1); the resulting plot is shown in figure(4.5). The results show that the worst case non-linearity error observed was less than 0.06%. Test was also conducted by varying the offset voltage V_{OS1} and bias current I_B of the opamp OA keeping the sensor resistance R_x constant at $9.78k\Omega$. Offset voltage of the opamp was emulated using a variable voltage source kept at the non-inverting terminal of the opamp, similar to the circuit equivalent shown in Figure(2.4). V_{OS1} was varied from -200 mV to 200 mV, in steps. The sensor resistance R_x was measured using the RDC for each value of offset voltage V_{OS1} .

Actual $k\Omega$	Measured $k\Omega$	% error (Full scale)	Actual $k\Omega$	Measured $k\Omega$	% error (Full scale)
1.19	1.23	-0.016	72.69	72.59	0.042
1.00	1.03	-0.015	82.62	82.53	0.038
2.70	2.739	-0.014	84.42	84.35	0.029
5.09	5.12	-0.012	94.16	94.07	0.038
9.97	10.00	-0.009	96.13	96.03	0.042
22.02	22.05	-0.013	99.74	99.55	0.080
27.00	26.99	0.004	100.23	100.15	0.033
30.24	30.23	0.004	125.01	125.13	-0.050
32.81	32.79	0.008	127.89	127.99	-0.042
35.47	35.45	0.008	142.72	142.77	-0.021
38.93	38.90	0.012	150.31	150.18	0.055
43.08	43.04	0.016	164.71	164.78	-0.029
51.35	51.31	0.016	200.91	200.75	0.067
53.40	53.34	0.025	219.65	219.50	0.063
62.62	62.57	0.021	200.90	200.76	0.059
68.40	68.31	0.038	220.10	219.98	0.050

Table 4.1 % error in reading

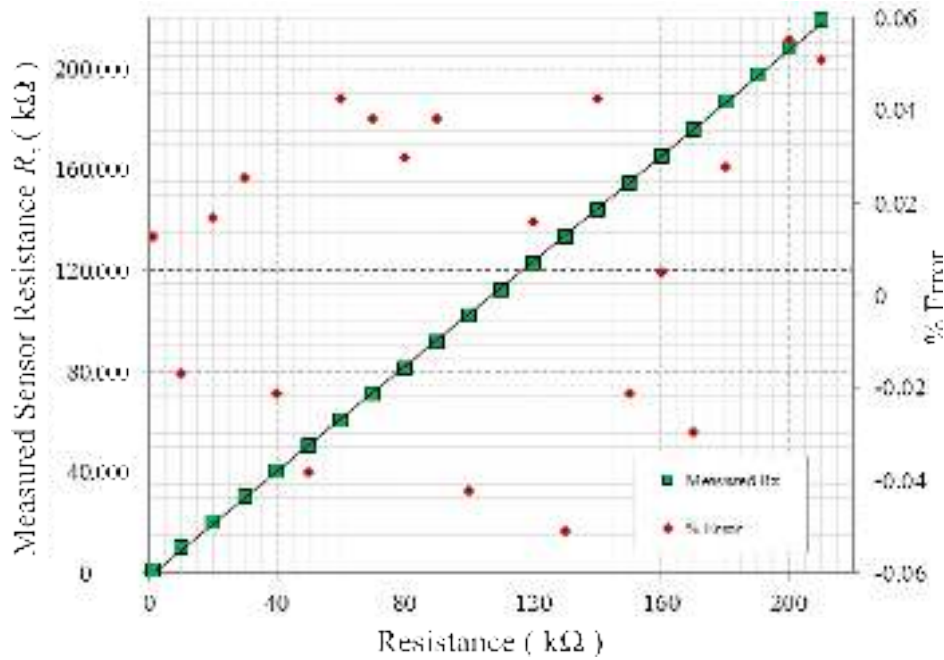


Fig. 4.5 Output and percentage error with change in resistance R_x .

The measured values were compared with their actual value and the % error was noted. The same is provided in Table(4.2), here deviation from the actual value of resistance R_x was used in calculating the percentage error

Offset Voltage(mV)	% Error in Reading	Bias Current(nA)	% Error in Reading
100	0.0080	100	0.0935
10	-0.0023	10	0.0975
0.1	-0.0023	1	0.0968
0.05	-0.0005	0.1	0.1053
-0.005	0.0005	-0.1	0.1163
-0.1	0.0035	-1	-0.0023
-10	-0.0015	-10	-0.0153
-100	-0.0142	-100	0.0935

Table 4.2 Effect of V_{OS1} and I_B

Similarly, a variable current source injecting a current I_B was introduced to the inverting terminal of opamp to realize a variable I_B . The % error in output was noted and tabulated for various values of bias current I_B in Table(4.2). The results show very good agreement with their actual values of the sensor resistance R_x with a worst case error less than 0.09%. figure(4.6). shows the waveform obtained from prototype for sensor resistance $R_x = 9.78k\Omega$ with the presence of an offset voltage $V_{OS1} = -200mV$ and bias current $I_B = -100nA$. The count noted was $N_1 = 13350$ and $N_2 = 9144$. As expected, they were not equal. The sensor resistance R_x computed using(2.7), was still accurate. This shows that, the proposed RDC shows high immunity to the offset voltage and bias current of the opamp.

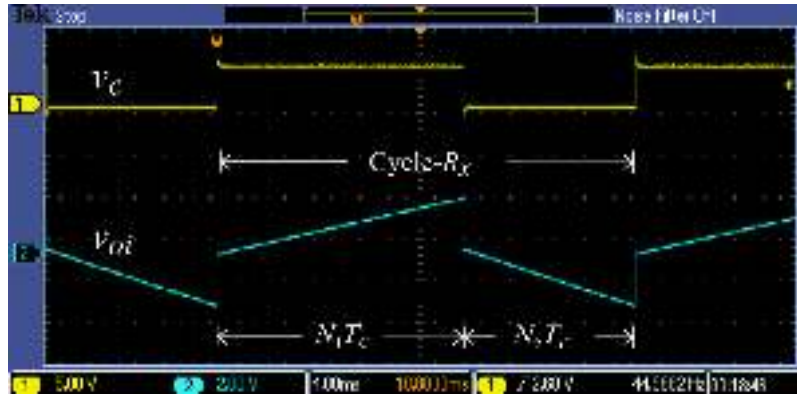


Fig. 4.6 Snap-shot of the oscilloscope screen showing the comparator output v_C and integrator output v_{oi} when an offset voltage $V_{OS1} = -200mV$ and bias current $I_B = -100nA$ are applied to the prototype developed

4.3 PCB Design and Fabrication

A dual layer PCB has been designed and components mounted on that as shown in Figure(4.7). A provision for connecting external reference voltage is also provided. Initially Arduino IDE used for the serial communication of the sensor value. After connecting the Bluetooth device as shown in the PCB Arduino is removed and the android application developed was used for taking the readings. PCB layouts, both top layer and bottom layer, are attached as Appendix-B.



Fig. 4.7 Components mounted on double layer PCB

4.4 Temperature test

A simulation conducted for the proposed prototype by adding noise component of each element of the prototype, by calculating R_x , it is found that the error produced is negligible. The experimental setup is as shown in figure(4.8) in which Lm35 from Texas Instruments used as temperature sensor and virtual instrumentation tool Lab View used to measure the sensor value for the corresponding temperature. Temperature increased up to 100° for a fixed value of sensor resistance and found that error is negligible. Corresponding screen shot obtained on the lab View is shown in figure(4.9) where waveform chart2 represents corresponding temperature for resistance value shown in waveform chart.

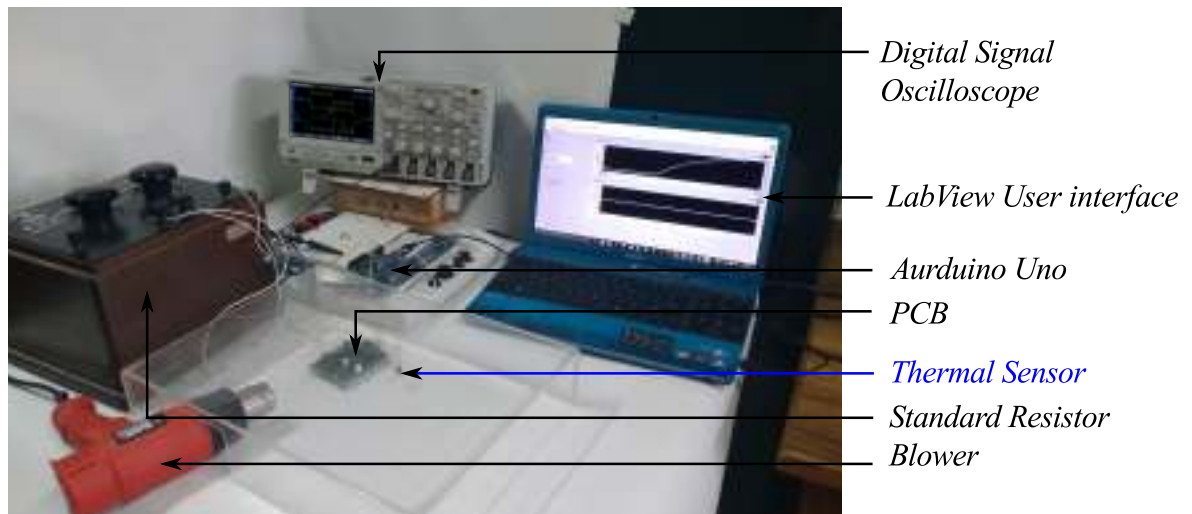


Fig. 4.8 Temperature test conducted in the laboratory

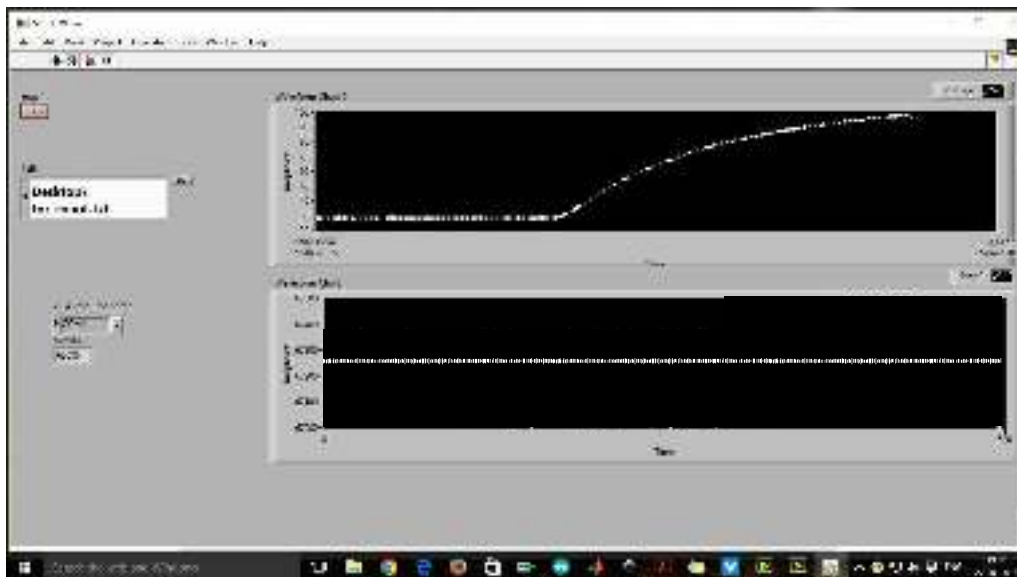


Fig. 4.9 Lab View screen shot

CHAPTER 5

CONCLUSION

5.1 SUMMARY OF THE WORK

A new Resistance-to-Digital (RDC) converter whose output is inherently insensitive to the circuit parameters such as offset voltage, bias current, gain of the amplifier, mismatch in the values of the reference voltages used, etc. has been developed and details are presented in the paper. The paper also presents the results of various tests conducted on the prototype RDC developed. From the test results, it has been noted that the output characteristic of the RDC is linear and sensitivity of the output towards various circuit parameters is negligible, as expected. This RDC will be very useful to interface single element resistive sensors to any digital system, especially when the measurement environment is expected to subject for large variations such as temperature that could affect various circuit parameters. Even in such a situation, the proposed RDC output will be reliable as its sensitivity of output to the circuit parameters is negligible

5.2 FUTURE WORK

The circuit in its present form has been tested with the help of a standard resistance box from as replacement for the sensor coil. Circuit output has shown highly linear and accurate characteristics with respect to the circuit parameters changed manually for the experiment purpose.

The circuit will be very useful for resistive sensors whose resistance vary linearly with the measurand. It can also be interfaced with existing resistive sensors for better performance as the output does not contain any contribution from usual circuit parameters. The same may be tested by integrating it with any of the existing Linear Resistive.

REFERENCES

- [1] E. O. Doebelin, *Measurement Systems—Application and Design*, 5th ed. New York: McGraw-Hill, 2004.
- [2] T. Nohara, “Resistance-to-digital converter”, U.S. Patent 008 576 7A1, May 8, 2003.
- [3] A. Flammini, D. Marioli and A. Taroni, “A low-cost interface to high-value resistive sensors varying over a wide range”, *IEEE Trans. Instrum. Meas.*, vol. 53, no. 4, pp. 1052 -1056, 2004.
- [4] Hoon Kim, Won-Sup Chung, Hee-Jun Kim, Sang-Hee Son, “A resistance deviation to pulsewidth converter for resistive sensors”, *IEEE Trans. Instrum. Meas.*, vol. 58, no. 2, Feb. 2009, pp. 397-400.
- [5] S. Kaliyugavaradhan, “A linear resistance-to-time converter with high resolution”, *IEEE Trans. Instrum. Meas.*, vol. 49, no. 1, pp. 151-153, Feb. 2000.
- [6] N. M. Mohan, B. George, V. J. Kumar, “Analysis of a Sigma–Delta Resistance-to-Digital Converter for Differential Resistive Sensors”, *IEEE Trans. Instrum. Meas.*, vol. 58, no. 5, pp. 1617-1622, May 2009.
- [7] E. W. Owen, “An integrating analog-to-digital converter for differential transducers”, *IEEE Trans. Instrum. Meas.*, vol. 28, no. 3, pp. 216–220, Sep. 1979.
- [8] N. M. Mohan, B. George, V. J. Kumar, “A Novel Dual-Slope Resistance-to-Digital Converter”, *IEEE Trans. Instrum. Meas.*, vol. 59, no. 5, pp. 1013-1018, May 2010.
- [9] F. Reverter and O. Casas, “Interfacing differential resistive sensors to micro-controllers: A direct approach”, *IEEE Trans. Instrum. Meas.*, vol. 58, no. 10, pp. 3405–3410, Oct. 2009.
- [10] Texas Instruments, “LM385-1.2”, <http://www.ti.com/lit/ds/symlink/lm185-adj.pdf>
<http://www.ti.com/lit/ds/symlink/lm185-adj.pdf>

- [11] Texas Instruments,“OP07”,<http://www.ti.com/lit/ds/symlink/op-07-n.pdf>
- [12] Texas Instruments,“LF347”,<http://www.ti.com/lit/ds/snosbh1d/snosbh1d.pdf>
- [13] Texas Instruments,“LM311”,<http://www.ti.com.cn/cn/lit/ds/symlink/lm311.pdf>
- [14] maxim integrated,“MAX4709”,<http://datasheets.maximintegrated.com/en/ds/MAX4708-MAX4709.pdf>
- [15] maxim integrated,“MAX4053”,<http://pdfserv.maximintegrated.com/en/ds/MAX4051-MAX4053A.pdf>
- [16] Atmel,“Atmega-328”,http://www.atmel.com/images/atmel-8271-8-bit-avr-microcontroller_atmega48a-48pa-88a-88pa-168a-168pa-328-328p-datasheet-complete.pdf

APPENDIX A

C-CODE FOR PROGRAMMING ATMEGA328 MICROCONTROLLER

The program is written for serving the microcontroller as control and logic unit. Here the switch positions for choosing R_x , R_s , and R_c are controlled and accordingly the time intervals are measured which leads to the measurement of sensor value and the output is continuously transmitted and displayed on Android device.

```
#include <avr/io.h>
#include <avr/io.h>
#include <util/delay.h>
#include <avr/interrupt.h>
#include <math.h>
const int  buttonPin = 12;

float Tnull=0;
float Ta=0;
float Tb=0;
float Tc=0;
float Td1=0;
float Td2=0;
float Tr1=0;
float Tr2=0;
float ratio=0;
float Rs=24.110; //in kohm
float Rx=0; //in kohm

unsigned long interval=1000; // the time we need to wait
unsigned long previousMillis=0; // millis() returns an unsigned long.
```

```

void setup() {
    Serial.begin(9600);

    pinMode(buttonPin, INPUT);
    pinMode(8, OUTPUT);
    pinMode(9, OUTPUT);
    pinMode(10, OUTPUT);
}

void loop() {

    digitalWrite(8, LOW);        // switch S1 connected to Rx
    digitalWrite(9, LOW);
    digitalWrite(10, LOW);

    if ((unsigned long)(millis() - previousMillis) >= interval)
    {
        previousMillis = millis();
    }

    for (int i = 0; i < 5; i++)    //for taking the average
    {
again_0:
        if (digitalRead(buttonPin) == LOW)
        {
            Tnull=micros();
            goto again_1;
        }
        else
        {
            goto again_0;
        }
    }
}

```

```

again_1:
if (digitalRead(buttonPin) == HIGH)
{
    Ta=micros();
    goto again_2;
}
else
{
    goto again_1;
}

again_2:
if (digitalRead(buttonPin) == LOW)
{
    Tb=micros();
    goto again_3;
}
else
{
    goto again_2;
}

again_3:
if (digitalRead(buttonPin) == HIGH)
{
    Tc=micros();
    goto again_4;
}
else
{
    goto again_3;
}

```

```

again_4:

Td1=Tb-Ta;                                     //on time
Td2=Tc-Tb;                                     //off time
Tr1=Tr1+(2*Td1*Td2)/(Td1+Td2);
}

Tr1 = Tr1 / 5;

Ta=0;Tb=0; Tb=0;Td1=0;Td2=0;

digitalWrite(8, LOW);
digitalWrite(9, LOW);                         // switch S1 connected to Rs
digitalWrite(10, HIGH);

if ((unsigned long)(millis() - previousMillis) >= interval)
{
    previousMillis = millis();
}

for (int i = 0; i < 5; i++)
{

again1_0:
if (digitalRead(buttonPin) == LOW)
{
    Tnull=micros();
    goto again1_1;
}
else

```

```

{
    goto again1_0;
}

again1_1:
if (digitalRead(buttonPin) == HIGH)
{
    Ta=micros();
    goto again1_2;
}
else
{
    goto again1_1;
}

again1_2:
if (digitalRead(buttonPin) == LOW)
{
    Tb=micros();
    goto again1_3;
}
else
{
    goto again1_2;
}

again1_3:
if (digitalRead(buttonPin) == HIGH)
{
    Tc=micros();
    goto again1_4;
}
else

```

```

{
    goto again1_3;
}

again1_4:

Td1=Tb-Ta;
Td2=Tc-Tb;
Tr2=Tr2+(2*Td1*Td2)/(Td1+Td2);
}

Tr2 = Tr2 / 5;
ratio=(Tr2*100000)/Tr1;
Rx=(ratio*Rs)/100;//final sensor value

Serial.println("\nTr1\t\t\tTr2\t\t\tRx in ohm");
Serial.println("-----");
Serial.print(Tr1);
Serial.print("\t\t");
Serial.print(Tr2);
Serial.print("\t\t");
Serial.println(Rx);
Serial.println("*****");
Ta=0;Tb=0; Tb=0;Td1=0;Td2=0;Tr1=0;Tr2=0;
}

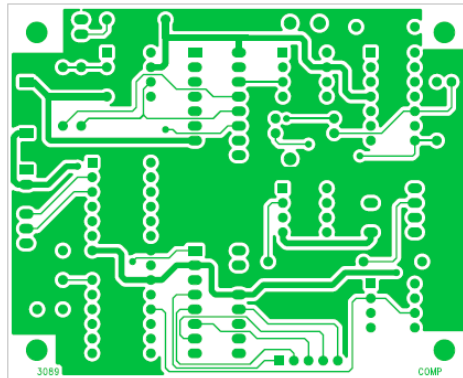
```


APPENDIX B

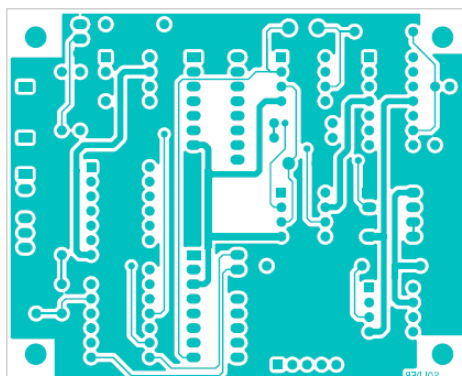
PCB LAYOUT

Solder and component sides of the PCB layout are as shown below:-

B.0.1 TOP LAYER



B.0.2 BOTTOM LAYER



CURRICULUM VITAE

Name : Semeerali.k
Date of Birth : 05 Nov 1990
Place of Birth : Mooniyoor, Kerala.
Education : B.Tech from College of Engineering, Trivandrum
Kerala University. 2013 Batch.
Work experience : Nill
E-mail : semeerali72@gmail.com